CFD Letters 16, Issue 4 (2024) 39-53

CFD Letters

Journal homepage:
https://semarakilmu.com.my/journals/index.php/CFD_Letters/index
ISSN: 2180-1363

Analysis of MHD and Heat Transfer Characteristics of Thermally Radiative Upper-Convected Maxwell Fluid Flow between Moving Plates: Semi-Analytical and Numerical Solution

Sampath Kumar V S[1], Devaki B[1], Nityanand P Pai[1,*]

[1] Department of Mathematics, Manipal Institute of Technology, Manipal Academy of Higher Education, Manipal, India

ARTICLE INFO

Article history:
Received 28 July 2023
Received in revised form 20 August 2023
Accepted 21 September 2023
Available online 1 January 2024

Keywords:
Upper-Convected Maxwell (UCM) Fluid; Heat transfer; MHD Flow; Thermal Radiation; Homotopy Perturbation Method (HPM); Finite Difference Method

ABSTRACT

The current paper studies the MHD and heat transfer characteristics of radiative upper-convected Maxwell fluid flow between two plates approaching or receding from each other with injection at the fixed lower porous plate. The governing momentum and energy equations are reduced into non-linear ordinary differential equations employing similarity transformations. With the help of the Homotopy Perturbation Method (HPM), an approximate analytic solution is obtained. This work aims to determine the effects of Reynolds number (R), Deborah number (De), Radiation parameter (Rd), Magnetic parameter (M), and Prandtl number (Pr) on the velocity and temperature profiles. It is observed that the Deborah number has a direct impact on the velocity profile when there is a squeezed flow. It is also observed that the magnetic parameter shows an indirect impact on the temporal distribution for both the upper plate moving away and towards the lower. The variations in the significant physical parameters on the coefficient of skin friction and heat transfer rates are also calculated. The results are then compared with the classical finite difference method and are in excellent agreement. It is found that larger the magnetic parameter, the dominance of viscous forces retards the velocity in the core region, and the increase in radiation parameter suppresses the heat transfer rates. This study is helpful in industrial applications, specifically in polymer processing.

1. Introduction

Analysing fluid transport phenomena in porous media is essential for many science and engineering applications. Fluid through a porous channel depends on Darcy's law. Due to the property of porous media to allow and resist the flow, it is pictured as a vital topic in the study of fluid mechanics. Moreover, it helps in better understanding of the behaviour of the fluid in real-world situations. The applications of porous materials are usually found in filters and water treatment systems to remove impurities from the fluids. Also, this concept is used in geology to study the movement of fluids through rocks and soil. Hence, the fluid flow through porous media becomes one of the most fascinating fields for researchers [1-3]. Berman [4] studied the laminar flow in porous

* *Corresponding author.*
E-mail address: nithyanand.pai@manipal.edu (Nityanand P Pai)

https://doi.org/10.37934/cfdl.16.4.3953

wall channels. Further, Yuan [5] continued the same work. The authors have dealt with the Newtonian fluid model in these papers.

Fluids are broadly classified into Newtonian and non-Newtonian fluids. The fluids that obey Newton's law of viscosity are known as Newtonian fluids. These fluids are the ideal fluids that do not exist in reality. Nevertheless, these fluids help in the basic understanding of nature. However, most of the fluids in nature are non-Newtonian. The diverse physical structure of non-Newtonian fluids cannot be expressed by a single rheological equation [6-13]. From the current information regarding the non-Newtonian fluids, the fluids are classified by rate, differential, and integral type fluid models. Rate-type non-Newtonian fluid models describe the mechanism of stress relaxation and retardation. Amongst such models, Maxwell fluid is the simplest one [14].

The Maxwell fluids are fluids that exhibit both elastic and viscous properties. The upper-convected Maxwell (UCM) fluid type represents the combined effects of inertia and viscoelasticity. UCM fluids have a broad scope in various industries, such as pharmaceutical, chemical, and food processing. Due to its viscoelasticity, its applications are found in lubricants, suspension formulations, and coatings. Due to their ability to maintain stable emulsions and suspend particles, these fluids are used as emulsifiers and thickeners in the chemical industry. Further, in the pharmaceutical industry, to control drug release rates, they are used in drug delivery systems.

The UCM fluid model is mainly used to explore the relaxation time of the fluid [15]. Fetecau *et al.,* [16] studied Stoke's second problem for Maxwell fluid flow. Vieru and Rauf [17] found an analytic solution for Stokes flow for Maxwell fluid, and further, the author [18] obtained solutions for Couette flows of Maxwell fluid using the Laplace transform technique. M L De Haro and others [19] analysed the Maxwell fluid flow in a rigid porous channel and gave some insight into the impact of elasticity on the dynamic permeability using the volume averaging method. Choi [20] investigated the Maxwell fluid flow in a porous channel through the power series method. Satish *et al.,* [21] explored the required time for the steady state of Maxwell fluid, and they also found the dependency of pressure on viscosity. Syed *et al.,* [22] examined the run-up fluid flow of the Maxwell model through the Laplace transformation method. Rana *et al.,* [23] obtained a solution for the UCM fluid flow in a porous medium considering suction/injection and extended it into a three-dimensional setup using the series method. Many authors have contributed significantly to the study of the Maxwell fluid with different geometries [24–27].

The study of MHD and heat transfer characteristics of fluid flow spans a range of scientific and engineering domains, including the petroleum industry, nuclear reactor, earth science, and metallurgy, specifically in the manufacturing process of polymers, artificial fibers, and thin films and many more [28-33]. Swati Mukhopadhyay [34] analysed the heat transfer profile of Maxwell fluid numerically using the shooting method. Ali *et al.,* [35] found an analytical and numerical solution for the effect of MHD and heat transfer in Maxwell fluid flow between two parallel plates. Zeeshan *et al.,* [36] found the exact solution for the UCM fluid flow in a porous channel with a source/sink immersed in it using the Homotopy analysis technique. Hayat [37] found the solution for the MHD flow of UCM fluid using a semi-analytical method. Further, the author extended his work to a rotating frame and found exact solutions using the Fourier sine transform method [38]. Raftari and Yildrim [39] gave the homotopy perturbation solution for the MHD UCM fluid flow above porous stretching sheets. Ilyas Khan *et al.,* [40] discussed some interesting results on the required time for the steady state of MHD Maxwell fluid in a porous half space. Anuj Kumar [41] presented an analytical solution and velocity profiles for electrically conducting UCM fluid in a porous medium.

Electromagnetic radiation generated by the particles in matter when there is an internal energy state transition is known as thermal radiation. It plays a critical role in the operations of many natural and man-made systems. The radiation properties are one of the most crucial process parameters in the thermal industry. The importance of thermal radiation emerges from the dependency on the heat flux quality of the final product in the polymer and the petroleum industry. Thermal radiation's impact on the construction of nuclear power plants, satellites, and a variety of complicated conversion systems is indeed crucial [42-44]. Hayat *et al.,* [45] described the exact solution for the impact of thermal radiation on MHD and heat transfer of Maxwell fluid in a porous medium using the homotopy analysis technique. Fazel and others [46] numerically analysed the impact of non-linear thermal radiation on MHD Maxwell fluid over a stretching sheet. Hosseinzadeh *et al.,* [47] did a numerical investigation of the non-linear thermal radiation effects of Maxwell fluid in a porous medium with a heated plate.

The MHD radiative squeezing flow of Maxwell fluid between porous plates is observed to have quite extensive applications. Various engineering and industrial applications such as petroleum transport, chemical processing, and metal casting employ these kinds of flows. Moreover, the potential applications of these flows are found in environmental and biomedical engineering. Due to its versatility, this flow can be modified to suit specific applications. It has become a valuable tool in several fields because of its ability to control flow patterns and fluid dynamics. However, it is found from the literature that the knowledge of the thermal radiation of the UCM fluid flow in a porous channel is limited. Hence, the study of MHD squeezing flow of a UCM fluid under radiation between parallel plates of which the lower plate is porous and fixed where the injection takes place is of interest in this work. This work attempted to study the thermal radiation effect on MHD and the temperature profile of UCM fluid flow between two plates, where the lower plate is fixed and porous, and the upper plate is moving with uniform velocity towards or away from the lower plate.

Most of the real-world problems are non-linear in nature. Obtaining solutions to these non-linear differential equations using the known analytical techniques is not possible. Hence, to obtain an approximate solution, numerical methods find scope in fluid mechanics [48-54]. FDM is one of the popular numerical methods in analysing many areas of science and technology. The abilities of FDM are confined when it comes to handling non-linear differential equations and require significant modification to do so. As numerical methods are very sensitive to grid size, FDM is prone to numerical instability that leads to inaccuracy and non-convergence in results. To overcome these challenges, researchers came up with the idea of semi-analytical methods. One such semi-analytical technique with broad scope is the Homotopy Perturbation method (HPM).

HPM is one of the promising modern analytical techniques to obtain solutions for non-linear problems in applied science and engineering. Ji-Huan He introduced, developed, and refined the HPM [55–57]. HPM can systematically generate a sequence of closed-form solutions that eventually converge to the exact solution with a higher convergence rate. This method overcomes the limitations of the traditional perturbation method and is helpful in solving a wide range of linear and non-linear problems [58–60]. HPM is more robust and has a broader scope in handling problems. Hence, this method can be applied to solve different class of problems and applications due to its flexibility.

2. Mathematical Formulation

Figure 1 shows the schematic diagram of the problem in two-dimensional cartesian coordinate system. Let u^* and v^* be the velocity components along x^* and y^* direction. The fluid model here considered is an incompressible electrically conducting UCM fluid. The fluid flow is between two plates located at $y^* = 0$ and $y^* = H$. The bottom plate is porous and stationary, and the upper plate is moving uniformly with a velocity V_w. A uniform magnetic field B_0 is applied along the y^* axis. Let τ

denote the extra stress tensor, μ_0 denote the low shear viscosity, λ_1 be the relaxation time, and γ be the rate of strain tensor. Then the stress strain relationship of Maxwell fluid is given by

$$\tau + \lambda_1 \hat{\tau} = \mu_0 \gamma \, . \tag{1}$$

The upper-convected time derivative of the stress tensor is defined as

$$\hat{\tau} = \frac{\partial \tau}{\partial t} + V\, \nabla\tau - (\nabla\tau)^{T}. \tag{2}$$

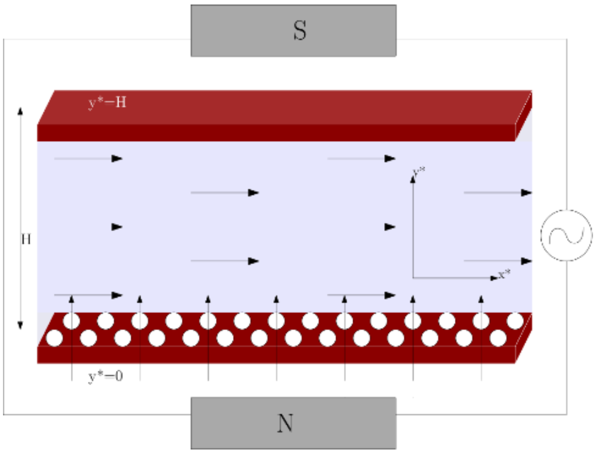

Fig. 1. Schematic diagram of the problem

Where t $(\;)^T$, V, and ∇v denotes the time, transpose vector, velocity vector, and fluid velocity gradient vector, respectively. The continuity and the momentum equations governing such type of flow are

$$\frac{\partial u^*}{\partial x^*} + \frac{\partial v^*}{\partial y^*} = 0. \tag{3}$$

$$u^* \frac{\partial u^*}{\partial x^*} + v^* \frac{\partial u^*}{\partial y^*} + \lambda \left[u^{*2} \frac{\partial^2 u^*}{\partial x^{*2}} + v^{*2} \frac{\partial^2 u^*}{\partial y^{*2}} + 2\, u^* v^* \frac{\partial^2 u^*}{\partial x^* \partial y^*} \right] = \nu \frac{\partial^2 u^*}{\partial x^* \partial y^*} - \frac{\sigma B_0}{\rho} u^*. \tag{4}$$

Ignoring the ohmic and viscous dissipation, the energy equation can be written as

$$u^* \frac{\partial T}{\partial x^*} + v^* \frac{\partial T}{\partial y^*} = \frac{k}{\rho\, C_p} \frac{\partial^2 T}{\partial y *^2} - \frac{1}{\rho\, C_p} \frac{\partial\, q_r}{\partial\, y^*}. \tag{5}$$

Where $\rho, \sigma,\, \nu,\, T(x^*, y^*),\, k,\, C_p$, and q_r are the fluid density, electrical conductivity of the fluid, kinematic viscosity, temperature at any point, thermal conductivity, specific heat, and radiation heat flux, respectively. The radiation heat flux q_r is defined using Rosseland approximation and is given by

$$q_r = -\frac{4\,\hat{\sigma}}{3\,\hat{k}} \frac{\partial\, T^4}{\partial\, y^*} \, , \tag{6}$$

Where $\hat{k}$ and $\hat{\sigma}$ denote the mean absorption coefficient and the Stefan-Boltzmann constant. With the assumption of temperature difference within the flow is such that T^4 may be expanded in a Taylor series and expanding T^4 about T_∞ and ignoring the higher orders, we obtain

$$T^4 \equiv 4\, T_\infty T - 3T^4{}_\infty \, . \tag{7}$$

Then the energy Eq. (5) becomes

$$u^* \frac{\partial T}{\partial x^*} + \ v^* \frac{\partial T}{\partial y^*} = \frac{k}{\rho\, C_p} \frac{\partial^2 T}{\partial y*^2} + \frac{16\, \hat{\sigma}\, T^3{}_\infty}{3\rho\, C_p\, \hat{k}} \ \frac{\partial^2 T}{\partial y*^2}\ . \tag{8}$$

The boundary conditions:

$$\text{At } y^* = 0: u^*(x^*, y^*) = 0, \quad v^*(x^*, y^*) = A.V_w, \quad T = T_w\ . \tag{9}$$
$$\text{At } y^* = H: u^*(x^*, y^*) = 0, \quad v^*(x^*, y^*) = V_w, \quad T = 0\ . \tag{10}$$

Here A is a constant parameter and $A < 0$ corresponds to injection process. T_w is the temperature at the lower plate. The dimensionless variables are presented as follow,

$$x = \frac{x^*}{H}; \quad y = \frac{y^*}{H}; \quad u^* = -V_w\, x\, f'(y). \tag{11}$$

From Eq. (3) and Eq. (4) we get

$$v^* = V_w\, f(y), \tag{12}$$

and

$$\theta = \frac{T}{T_w}\ . \tag{13}$$

Using the non-dimensional parameters in momentum and energy equations, we get

$$f\,'''' - M^2 f\,'' + R(f\,' f\,'' - f\, f\,''') + De(\,2\, f\,'^2 f\,'' + \,2\, f\, f\,''^2 - \, f^2 f\,''') = 0. \tag{14}$$
$$(1 + \tfrac{4}{3}\, Rd)\, \theta\,'' - R\, Pr\, f\, \theta\,' \ = 0. \tag{15}$$

With boundary conditions

$$f(0) = A, \quad f\,'(0) = 0,\ f(1) = 1, \quad f\,'(1) = 0, \quad \theta(0) = 1,\ \theta(1) = 0. \tag{16}$$

Where R, De, Rd, M and Pr represent the Reynolds number, Deborah number, Radiation parameter, magnetic parameter, and Prandtl number respectively are defined as

$$R = \frac{V_w\, H}{\upsilon}, \quad De = \frac{\lambda\, {V_w}^2}{\upsilon}, \quad M = \sqrt{\frac{\sigma\, B_0 H}{\mu}}, \quad Rd = \frac{4\, \hat{\sigma}\, T^3{}_\infty}{k\, \hat{k}}, \quad Pr = \frac{\mu\, C_p}{k}\ . \tag{17}$$

Here, $R > 0$ and $R < 0$ represent the situation of upper plate moving away from the bottom plate and upper plate approaching the lower plate, respectively.

3. Method of Solution

We obtain a system of non-linear ordinary differential equation (ODE) after applying similarity transformations. We adopt semi-analytical technique approach to get the solution and we use numerical technique to verify the obtained results. The system of non-linear ODEs along with the boundary conditions are solved using homotopy perturbation method (HPM). Obtained results are compared numerically using classical finite difference method. To narrate the HPM solution for the system of non-linear differential equations, let us take

$$D_1[f(\eta)] - f_1(\eta) = 0, \tag{18}$$
$$D_2[\theta(\eta)] - f_2(\eta) = 0. \tag{19}$$

Where D_1 and D_2 denotes the operators, $f(\eta)$ and $\theta(\eta)$ are unknown functions, η is the independent variable and f_1, f_2 are known functions. D_1 and D_2 can be written as,

$$D_1 = L_1 + N_1,$$
$$D_2 = L_2 + N_2.$$

Where L_1 and N_1 are the linear and non-linear parts of Eq. (18) and L_2 and N_2 are the linear and non-linear parts of Eq. (19). The homotopy equations are obtained by choosing proper linear and non-linear parts. The homotopy equations for Eq. (18) and Eq. (19) are

$$H_1\big(\phi_1(\eta, q; q)\big) = (1-q)[L_1(\phi_1, q) - L_1(v_0(\eta))] + q[D_1(\phi_1, q) - f_1(\eta)] = 0, \tag{20}$$
$$H_2\big(\phi_2(\eta, q; q)\big) = (1-q)[L_2(\phi_2, q) - L_2(v_0(\eta))] + q[D_2(\phi_2, q) - f_2(\eta)] = 0. \tag{21}$$

Here the initial guess to the Eq. (18) and Eq. (19) is v_0.

We assume the solution of Eq. (20) and Eq. (21) as

$$\phi_1(\eta, q) = \sum_{n=0}^{\infty} q^n f_n(\eta), \tag{22}$$
$$\phi_2(\eta, q) = \sum_{n=0}^{\infty} q^n \theta_n(\eta). \tag{23}$$

The solution to the considered problem is Eq. (22) and Eq. (23) at $q = 1$.

The zeroth, first, and second order solutions for the considered problem are as follows

$$f_0 = 2Ay^3 - 3Ay^2 + A - 2y^3 + 3y^2. \tag{24}$$

$$\begin{aligned} f_1 = -\frac{1}{420}(A-1)(y-1)^2 y^2 (4\,De\,(A^2(50y^5 - 125y^4 + 42y^3 + 104y^2 - 86y \\ +39) - A(100y^5 - 250y^4 + 84y^3 + 124y^2 - 88y + 15) + 50y^5 - 125y^4 \\ +42y^3 + 20y^2 - 2y - 24) + 3(2R(A(4y^3 - 6y^2 + 5y - 19) - 4y^3 + 6y^2 \\ -5y - 16) + 7(2y-1)M^2)). \end{aligned} \tag{25}$$

$$\begin{aligned} f_2 = \frac{1}{8408400}(-1+A)^2 y^2 [16De^2(243387 + 24576y + 24765y^2 + 24954y^3 - 191073y^4 + \\ 228678y^5 + 69279y^6 + 74330y^7 - 298997y^8 + 266250y^9 - 12100y^{10} + 2200y^{11} + \\ A(23937 + 48570y - 167037y^2 - 10272y^3 + 259606y^4 + 382760y^5 - 871164y^6 - \\ 230344y^7 + 1179244y^8 - 1065000y^9 + 484000y^{10} - 88000y^{11}) + A^4(-148149 + \\ 500324y - 818168y^2 + 265740y^3 + 939238y^4 - 1319050y^5 + 663327y^6 + 7354y^7 - \\ 282253y^8 - 1065000y^9 + 484000y^{10} - 88000y^{11}) - A^3(-53694 + 482506y\ldots)\ldots)]. \end{aligned} \tag{26}$$

$$\theta_0 = 1 - y. \tag{27}$$

$$\theta_1 = \frac{3}{20(4Rd+3)} (2\,A\,y^5\,Pr\,R - 5\,A\,y^5 Pr\,R + 10\,A\,y^2\,Pr\,R - 7\,A\,y\,Pr\,R - 2y^5\,Pr\,R + 5y^4\,Pr\,R - 3\,y\,Pr\,R). \tag{28}$$

$$\theta_2 = \frac{1}{92400(3+4Rd)} [2934DePrRy - 2862ADePrR\,y - 3078A62DePrRy + 3006A^3DePrRy - 99MPrRy - 99M2PrRy + 99AM^2PrRy + 3432PrR^2y + 66APrR^2y - 3498A^2PrR^2y + 264Pr^2R^2 - 28248APrR^2y - 41316A^2Pr^2R^2\,y + 3912DePrRRdy - 3816ADePrRRd\,y - 4104A^2DePrRRdy + 4008A^3DePrRRd - 132M^2PrRRdy + 132AM^2PrRRd\,y + 4576PrR^2Rdy + 88APrR^2Rdy - \dots]. \tag{29}$$

4. Results and Discussion

This section discusses the injection case of MHD UCM flow and heat transfer characteristics between two plates by considering the effect of thermal radiation. In this model, the plate in the bottom is porous and stationary and the upper plate is set in motion (approaching or receding from the lower plate) with a uniform velocity V_w. The effect of pertinent parameters such as Reynolds number, Deborah number, Radiation parameter, Magnetic parameter, and Prandtl number on fluid flow and temperature fields are illustrated using graphs (Figure 2 - Figure 15), and skin friction coefficient $(f''(0), f''(1))$ and heat transfer rates $(\theta'(0), \theta'(1))$ are also computed and given in tables (Table 1 and Table 2).

The effect of R, the parameter which characterizes the movement of the upper plate on the velocity field, is shown in Figure 2, and it is found to be increasing when the upper plate is approaching the bottom one $(R < 0)$ in the region $0 \leq y \leq 0.5$ and found to be decreasing in the $0.5 \leq y \leq 1$ region. In the case of the upper plate moving away from the bottom plate ($R > 0$), an opposite behaviour is observed. It is observed that in both the cases, the velocity curve exhibits parabolic nature. Figure 3 and Figure 4 illustrate the impact of magnetic parameter (M) on the velocity field for $R = 2$ and $R = -2$, respectively. It is observed that, in the core region the velocity is retarding for increment in M. This indicates the fact of increment in M produces Lorentz force, which shrinks the boundary layer thickness. The effect of magnetic field causes a damping effect on the velocity by creating a drag force which opposes the motion there by supressing the velocity.

In Figure 5 and Figure 6, it is observed that the impact of De on the velocity profiles for $R = 5$ and $R = -5$, resulting in a parabolic curve. The Maxwell parameter De is the ratio of relaxation time to the characteristic time of the deformation phenomena. Deborah number distinguishes how a particular material will behave over a given time frame and is related to the unsteadiness of the flow. Deborah number depends upon retardation time. Physically, a large λ_1 (retardation time) of any substance makes the fluid less viscous. Here $De = 0$ represents the velocity curve for the Newtonian case. Higher the De value stronger the elastic behaviour, and the flattening of the boundary layer. From Figure 5, it is noted that the velocity decreases for increment in De in the region $0 \leq y \leq 0.65$. An enhancement in the velocity is observed in $0.65 \leq y \leq 1$ region. For $R = -5$ case also the velocity is found to be decreasing in the range $0 \leq y \leq 0.79$ and increasing in the region $0.79 \leq y \leq 1$.

Figure 7 represents the temperature variation for different values of R. When the upper plate is approaching the fixed bottom plate, the temperature increases for an increased value of R. Whereas for the $R > 0$ case, an opposite trend is observed. A linear relation is noted for low Reynolds numbers in both cases. Figure 8 and Figure 9 depict the effect of M on $\theta(y)$ for $R = 2$ and $R = -2$.

A linear relation can be noted from these graphs. From the figure, it is observed that the temperature decrement for increased values of M is due to the weaker Lorentz force. The impact of the parameter De on the temperature profile is illustrated in Figure 10 and Figure 11 for $R = 1$ and $R = -1$ cases, respectively. In Figure 10, it is observed that the temperature enhances as De increased, indicating that the higher relaxation time, results in higher temperature. From the figure, it is also observed the shear thickening behaviour of Maxwell fluid. Figure 11 illustrates $R = -1$ case, where an opposite trend is observed in the case of $R = 1$.

Figure 12 and Figure 13 demonstrate the variation of Pr on the temperature field for $R = 2$ and $R = -2$, respectively. The Prandtl number (Pr) is a ratio of momentum diffusivity to thermal diffusivity. As temperature rises, the velocity boundary layer becomes larger than that of the thermal boundary layer. This implies that as Pr increases, the thermal boundary layer decreases. Physically, a larger value of Pr results in less thermal capacity. Therefore, in Figure 12, the temperature was found to be increasing for increment in Pr. An opposite trend is noted for the squeezing case. Figure 14 and Figure 15 depict the effect of radiation parameter Rd on the temperature profile for the cases $R = 2$ and $R = -2$. A linear relation is observed in both cases. The mean absorption coefficient is found to be reducing for higher thermal radiation parameter Rd, which is responsible for enhanced heat transfer. As a result, the temperature distribution increases for increased values of Rd in Figure 14. An opposite behaviour is observed in $R = -2$ case.

Table 1 shows the variation of heat transfer rates for different values of R and Rd. When the radiation parameter Rd is increased, the heat transfer rate decreases in both cases. From the table, it is clear that in the case of the upper plate moving away from the lower plate, the heat transfer rate $\theta'(0)$ was enhanced and $\theta'(1)$ suppressed. An opposite trend is observed for $R < 0$ case. Table 2 gives the skin friction coefficient values at the lower ($f''(0)$) and upper plate ($f''(1)$) for the injection case. We observe that, when the upper plate moves away from the bottom plate, the skin friction at the lower and upper plates decreases, whereas it is enhanced in the case of plates moving closer. It is noted that as there is an increment in M, $f''(0)$ is increasing, and $f''(1)$ is decreasing. The values of $f''(0)$ and $f''(1)$ are suppressed for increased values of De.

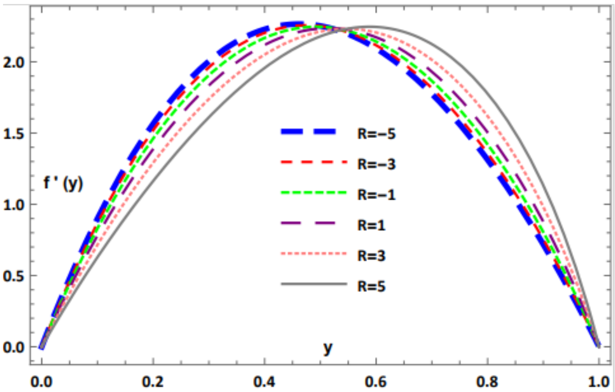

Fig. 2. $f'(y)$ for different R when $M = 1, De = 0.3$

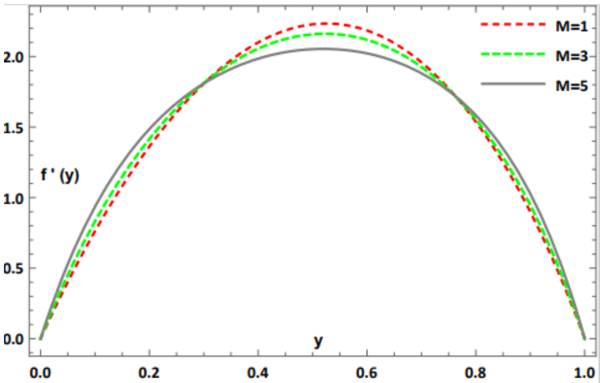

Fig. 3. $f'(y)$ for different M when $R = 2, De = 0.1$

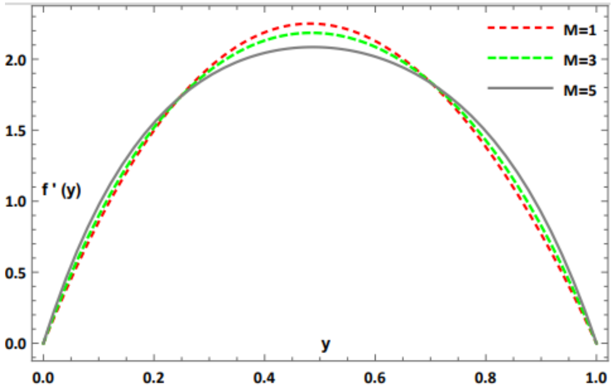

Fig. 4. $f'(y)$ for different M when $R = -2, De = 0.1$

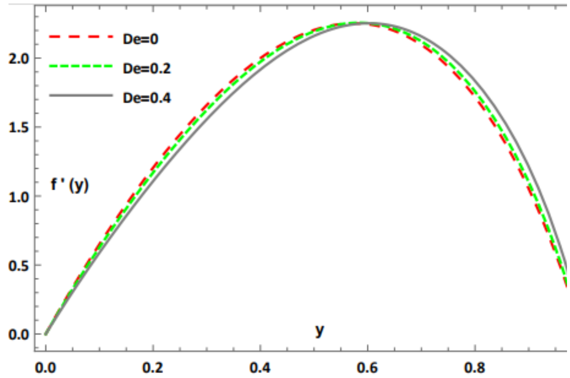

Fig. 5. $f'(y)$ for different De when $R = 2, M = 0.5$

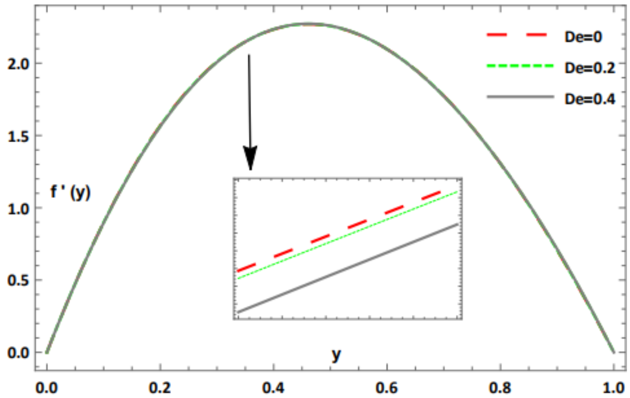

Fig. 6. $f'(y)$ for different De when R=-2, $M = 0.5$

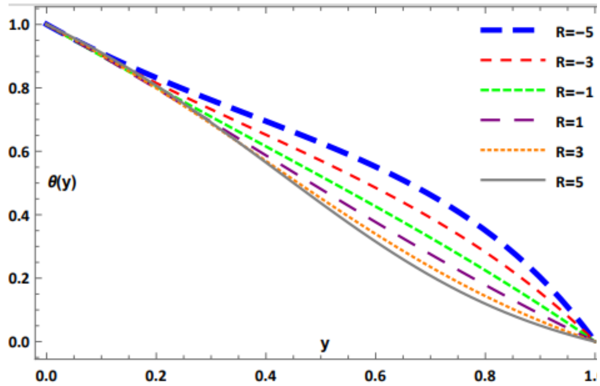

Fig. 7. $\theta(y)$ for different R when $M = 0.5, Rd = 0.1, De = 0.1, Pr = 0.5$

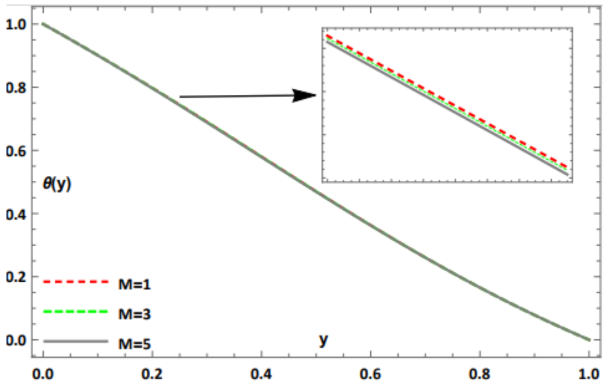

Fig. 8. $\theta(y)$ for different M when $R = 2, Rd = 0.1, De = 0.1, Pr = 0.5$

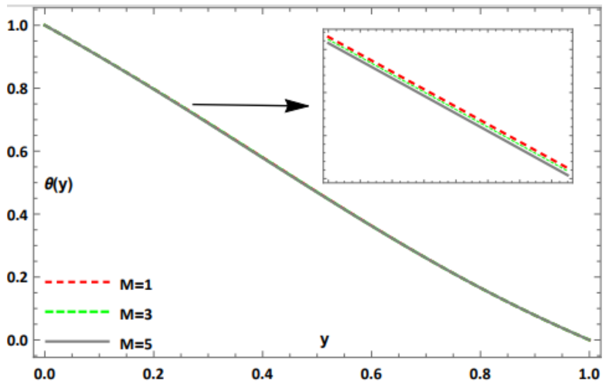

Fig. 9. $\theta(y)$ for different M when $R = -2, Rd = 0.1, De = 0.1, Pr = 0.5$

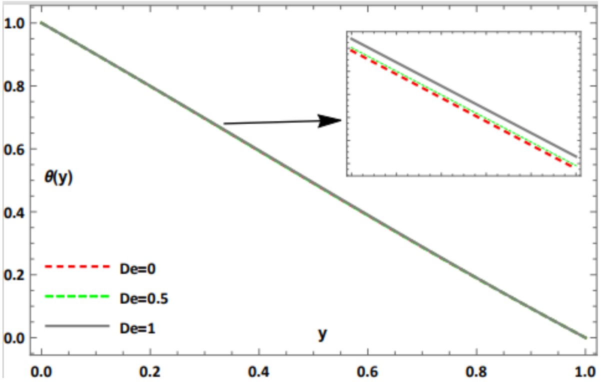

Fig. 10. $\theta(y)$ for different De when $R = 2, Rd = 0.2, M = 0.5, Pr = 0.4$

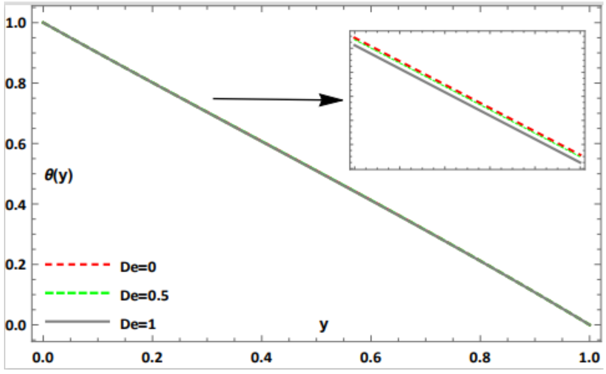

Fig. 11. $\theta(y)$ for different De when $R = -2, Rd = 0.2, M = 0.5, Pr = 0.4$

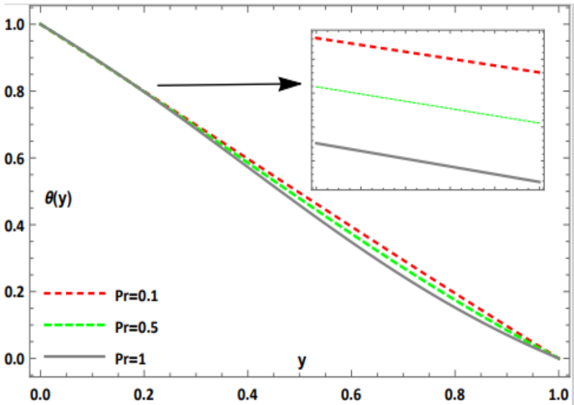

Fig. 12. $\theta(y)$ for different Pr when $R = 2, Rd = 0.2, M = 0.5, De = 0.2$

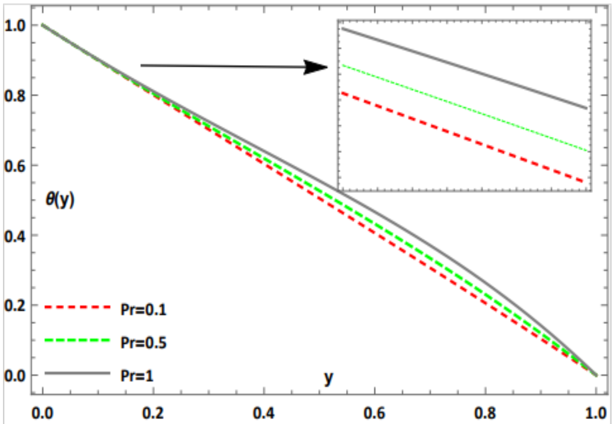

Fig. 13. $\theta(y)$ for different Pr when $R = -2, Rd = 0.2, M = 0.5, De = 0.2$

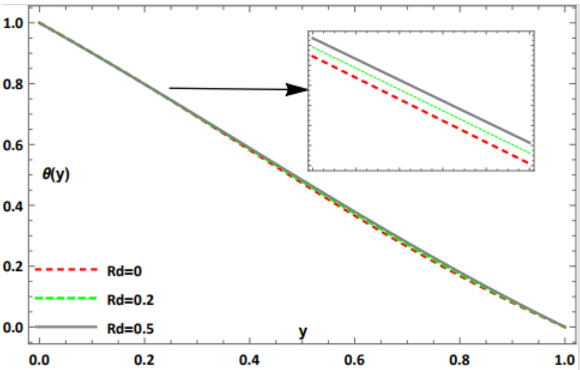

Fig. 14. $\theta(y)$ for different Rd when $R = 1, Pr = 0.4, M = 0.5, De = 0.2$

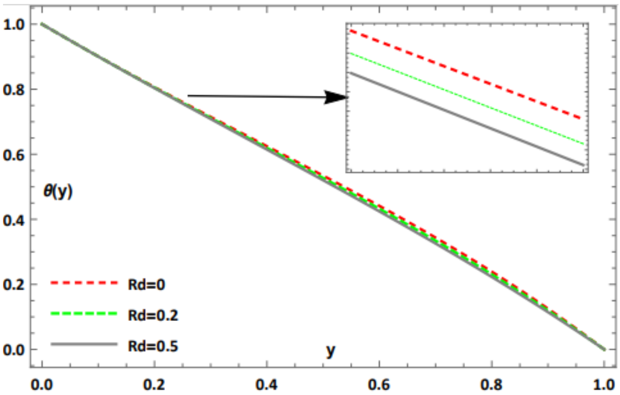

Fig. 15. $\theta(y)$ for different Rd when $R = -1, Pr = 0.4, M = 0.5, De = 0.2$

Table 1
Injection: heat transfer rate for A = −0.5, De = 0.1

R	Rd	$\theta'(0)$		$\theta'(1)$	
		HPM	FDM	HPM	FDM
-5	0.1	-0.980829	-0.988605	-0.840872	-0.835683
-1		-0.98431	-0.98362	-0.84048	-0.84041
1		-0.98072	-0.98003	-0.84439	-0.843925
5		-0.96977	-0.96787	-0.85552	-0.85489
-5	0.3	-0.99165	-0.99060	-0.86543	-0.86464s
-1		-0.98725	-0.98652	-0.86936	-0.86857
1		-0.98464	-0.983578	-0.872282	-0.871501
5		-0.9757	-0.97460	-0.88153	-0.88077
-5	0.6	-0.99317	-0.99206	-0.88584	-0.88496
-1		-0.98973	-0.98860	-0.88920	-0.88833
1		-0.98724	-0.98613	-0.89171	-0.89084
5		-0.97967	-0.97853	-0.89996	-0.89876

Table 2
Injection: skin friction coefficient for A = −0.5

R	De	$M = 1$			
		$f''(0)$		$f''(1)$	
		HPM	FDM	HPM	FDM
-5	0.1	10.13780	10.12750	-7.63383	-7.62759
-1		9.38681	9.34772	-8.82480	-8.78904
1		8.83570	8.79854	-9.84952	-9.80362
5		7.11056	7.05162	-13.67460	-13.49480
-5	0.3	10.15610	9.73890	-7.69700	-7.48223
-1		9.36468	8.96130	-9.01940	-8.70534
1		8.76743	8.39115	-10.31480	-9.79176
5		6.84428	6.55710	-15.15890	-14.00460
-5	0.6	10.76070	9.77131	-7.12739	-6.59100
-1		10.18460	9.21907	-8.06629	-7.40394
1		8.61747	8.38207	-11.72620	-11.22110
5		6.28049	5.73695	-19.89120	-15.42500
		$M = 3$			
-5	0.1	10.93940	10.89130	-8.57775	-8.58607
-1		10.42870	10.38050	-10.00330	-9.95771
1		10.06930	10.02120	-11.07330	-11.01550
5		9.02554	8.98036	-14.52200	-14.41870
-5	0.3	10.95580	10.77620	-8.65544	-8.71970
-1		10.25460	10.23550	-10.32390	-10.30340
1		10.01260	9.86512	-12.03990	-11.58060
5		8.87193	8.70601	-16.20890	-15.70890
-5	0.6	10.97090	10.40860	-9.40676	-8.92957
-1		10.34850	10.40860	-11.79360	-8.92957
1		10.34850	10.05230	-11.79360	-11.35160
5		8.52781	8.09945	-21.45070	-18.97440

5. Conclusions

The current research work aims to provide the significance of MHD and radiation effects on UCM Maxwell fluid flow between moving plates. Following observations are made from the above study:

i. Increase in magnetic effect supresses the velocity field in the core region for both $R > 0$ and $R < 0$.
ii. As the plates move towards each other, velocity is found to be increasing in the range $0 \leq y \leq 0.55$ and decreasing in the range $0.55 \leq y \leq 1$, whereas an opposite trend is observed in case of plates moving away from each other.
iii. When the plates are moving apart from each other, an increment in Deborah number results decrease in velocity till the point of inflection $y = 0.6$ and an increment is observed after the point of inflection. Trend is found to be in opposite for the case plates moving close to each other.
iv. Temperature field is observed to be decreasing with increase in magnetic field for both $R > 0$ and $R < 0$.
v. Increase in De and Rd resulted in an increment in the temperature fields for $R > 0$, whereas an opposite behaviour is noted for $R < 0$.
vi. As the plates move away, increase in Prandtl number suppresses the temperature filed profile and the trend is found to be in opposite nature for $R < 0$ case.
vii. The effect of various physical parameters on skin friction and heat transfer rates are also calculated. The results are compared with numerical values obtained using finite difference method and found to be in good agreement.
viii. Increase in Reynolds number supresses the skin friction coefficient on the lower plate, whereas the magnitude increases on the upper plate.
ix. Increase in magnetic parameter resulted in increase in the magnitude of coefficient of skin friction on both upper and lower plates.
x. As the radiation parameter increases, the magnitude of heat transfer rate increases for both plates moving towards and away from each other.

Acknowledgement
This research was not funded by any grant. Authors thank the Manipal Academy of Higher Education, Manipal for their constant support throughout the research.

References

[1] Hosseinzadeh, S., Hosseinzadeh, Kh., Hasibi, A., and Ganji, D.D. "Thermal analysis of moving porous fin wetted by hybrid nanofluid with trapezoidal, concave parabolic and convex cross sections." *Case Studies in Thermal Engineering 30*, (2022): 101757. https://doi.org/10.1016/j.csite.2022.101757
[2] Talebi Rostami, H., M. Fallah Najafabadi, Kh Hosseinzadeh, and D. D. Ganji. "Investigation of mixture-based dusty hybrid nanofluid flow in porous media affected by magnetic field using RBF method." *International Journal of Ambient Energy* 43, no. 1 (2022): 6425-6435. https://doi.org/10.1080/01430750.2021.2023041
[3] Abdollahi, S.A., Jalili, P., Jalili, B., Nourozpour, H., Safari, Y., Pasha, P., and Ganji, D.D. "Computer simulation of Cu: AlOOH/water in a microchannel heat sink using a porous media technique and solved by numerical analysis AGM and FEM." *Theoretical and Applied Mechanics Letters 13*, no. 3 (2023): 100432. https://doi.org/10.1016/j.taml.2023.100432
[4] Berman, Abraham S. "Laminar flow in channels with porous walls." *Journal of Applied physics* 24, no. 9 (1953): 1232-1235.

[5] Yuan, S.W. "Further Investigation of Laminar Flow in Channels with Porous Walls." *Journal of Applied Physics* 27, no. 3 (1956): 267–269. http://dx.org/10.1063/1.1722355

[6] Eldabe, N., Abouzeid, M., and Ali, H. "Effect of Heat and Mass Transfer on Casson Fluid Flow Between Two Co-Axial Tubes with Peristalsis." *Journal of Advanced Research in Fluid Mechanics and Thermal Sciences 76*, no. 1 (2020): 54–75. https://doi.org/10.37934/arfmts.76.1.5475

[7] Abuiyada, Alaa Jaber, Nabil Tawfik Eldabe, Mohamed Yahya Abou-zeid, and Sami Mohamed El Shaboury. "Effects of thermal diffusion and diffusion thermo on a chemically reacting MHD peristaltic transport of Bingham plastic nanofluid." *Journal of Advanced Research in Fluid Mechanics and Thermal Sciences* 98, no. 2 (2022): 24-43.https://doi.org/10.37934/arfmts.98.2.2443

[8] Mohamed, Yasmeen Mostafa, Nabil Tafik El-Dabe, Mohamed Yahya Abou-Zeid, Mahmoud Elhassan Oauf, and Doaa Roshhdy Mostapha. "Peristaltic Transport of Carreau Coupled Stress Nanofluid with Cattaneo-Christov Heat Flux Model Inside a Symmetric Channel: Peristaltic transport of Carreau coupled stress nanofluid." *Journal of Advanced Research in Fluid Mechanics and Thermal Sciences* 98, no. 1 (2022): 1-17. https://doi.org/10.37934/arfmts.98.1.117

[9] Najafabadi, M. Fallah, H. TalebiRostami, Kh Hosseinzadeh, and D. D. Ganji. "Investigation of nanofluid flow in a vertical channel considering polynomial boundary conditions by Akbari-Ganji's method." *Theoretical and Applied Mechanics Letters* 12, no. 4 (2022): 100356. https://doi.org/10.1016/j.taml.2022.100356

[10] Zangooee, M. R., Kh Hosseinzadeh, and D. D. Ganji. "Hydrothermal analysis of hybrid nanofluid flow on a vertical plate by considering slip condition." *Theoretical and Applied Mechanics Letters* 12, no. 5 (2022): 100357. https://doi.org/10.1016/j.taml.2022.100357

[11] Abuiyada, Alaa, Nabil Eldabe, Mohamed Abouzeid, and Samy Elshaboury. "Influence of Both Ohmic Dissipation and Activation Energy on Peristaltic Transport of Jeffery Nanofluid through a Porous Media." *CFD Letters* 15, no. 6 (2023): 65-85. https://doi.org/10.37934/cfdl.15.6.6585

[12] Hosseinzadeh, Kh, M. R. Mardani, M. Paikar, A. Hasibi, T. Tavangar, M. Nimafar, D. D. Ganji, and Mohammad Behshad Shafii. "Investigation of second grade viscoelastic non-Newtonian nanofluid flow on the curve stretching surface in presence of MHD." *Results in Engineering* 17 (2023): 100838.. https://doi.org/10.1016/j.rineng.2022.100838

[13] Zhou, Jincheng, As' ad Alizadeh, Masood Ashraf Ali, and Kamal Sharma. "The use of machine learning in optimizing the height of triangular obstacles in the mixed convection flow of two-phase MHD nanofluids inside a rectangular cavity." *Engineering Analysis with Boundary Elements* 150 (2023): 84-93. https://doi.org/10.1016/j.enganabound.2023.02.002

[14] Maxwell, J Clerk., "On the Dynamical Theory of Gases." *Philosophical Transactions of the Royal Society of London* 157, (1867): 49–88.

[15] Olsson, Fredrik, and Jacob Yström. "Some properties of the upper convected Maxwell model for viscoelastic fluid flow." *Journal of non-newtonian fluid mechanics* 48, no. 1-2 (1993): 125-145. https://doi.org/10.1016/0377-257(93)80068-M

[16] Fetecau, C., M, J., Fetecau, C., and I, S. "A note on the second problem of Stokes for Maxwell fluids." *International Journal of Non-Linear Mechanics* 44, no. 10 (2009): 1085–1090. https://doi.org/10.1016/j.ijnonlinmec.2009.08.003

[17] Vieru, Dumitru, and Abdul Rauf. "Stokes flows of a Maxwell fluid with wall slip condition." *Canadian Journal of Physics* 89, no. 10 (2011): 1061-1071. https://doi.org/10.1139/p11-099

[18] Vieru, Dumitru, and Azhar Ali Zafar. "Some Couette flows of a Maxwell fluid with wall slip condition." *Appl Math Inf Sci* 7 (2013): 209-219. https://doi.org/10.12785/amis/070126

[19] De Haro, M. López, J. A. P. Del Río, and S. Whitaker. "Flow of Maxwell fluids in porous media." *Transport in Porous Media* 25 (1996): 167-192. https://doi.org/10.1007/BF00135854

[20] Choi, J. J., Zvi Rusak, and J. A. Tichy. "Maxwell fluid suction flow in a channel." *Journal of non-newtonian fluid mechanics* 85, no. 2-3 (1999): 165-187. https://doi.org/10.1016/S0377-0257(98)00197-9

[21] Karra, Satish, Vít Průša, and K. R. Rajagopal. "On Maxwell fluids with relaxation time and viscosity depending on the pressure." *International Journal of Non-Linear Mechanics* 46, no. 6 (2011): 819-827. https://doi.org/10.1016/j.ijnonlinmec.2011.02.013

[22] Qadri, Syed Yedulla, and M. Veera Krishna. "Run-Up Flow of a Maxwell Fluid through a Parallel Plate Channel." *American Journal of computational mathematics* 2013 (2013). https://doi.org/10.4236/ajcm.2013.34039

[23] Rana, M. A., Y. Ali, and M. Shoaib. "Three-dimensional flow of an upper convected Maxwell fluid between two horizontal parallel porous plates with periodic injection/suction." In *2017 14th International Bhurban Conference on Applied Sciences and Technology (IBCAST)*, pp. 561-568. IEEE, 2017. https://doi.org/10.1109/IBCAST.2017.7868107

[24] Sadeghy, Kayvan, Amir-Hosain Najafi, and Meghdad Saffaripour. "Sakiadis flow of an upper-convected Maxwell fluid." *International Journal of Non-Linear Mechanics* 40, no. 9 (2005): 1220-1228. https://doi.org/10.1016/j.ijnonlinmec.2005.05.006

[25] Hafeez, Hafeez Y., and Chifu E. Ndikilar. "Flow of viscous fluid between two parallel porous plates with bottom injection and top suction." *Progress in physics* 10, no. 1 (2014): 49-51.https://www.ptep-online.com/2014/PP-36-4.PDF

[26] Wang, Shaowei, Peilin Li, and Moli Zhao. "Analytical study of oscillatory flow of Maxwell fluid through a rectangular tube." *Physics of Fluids* 31, no. 6 (2019). https://doi.org/10.1063/1.5100220

[27] Haroon, Tahira, Abdul Majeed Siddiqui, Hameed Ullah, and Dianchen Lu. "Flow of Maxwell fluid in a channel with uniform porous walls." *Journal of Applied Analysis and Computation* 11, no. 3 (2021): 1322-1347. https://doi.org/10.11948/20200158

[28] Bahambary, Khashayar Rahnamay, and Brian Fleck. "A study of inflow parameters on the performance of a wind turbine in an atmospheric boundary layer." *Journal of Advanced Research in Numerical Heat Transfer* 11, no. 1 (2022): 5-11.

[29] Bajuri, Muhammad Nur Arham, Djamal Hissein Didane, Mahamat Issa Boukhari, and Bukhari Manshoor. "Computational Fluid Dynamics (CFD) Analysis of Different Sizes of Savonius Rotor Wind Turbine." *Journal of Advanced Research in Applied Mechanics* 94, no. 1 (2022): 7-12.

[30] Jalili, B., A. Mousavi, Payam Jalili, Amirali Shateri, and D. Domiri Ganji. "Thermal analysis of fluid flow with heat generation for different logarithmic surfaces." *International Journal of Engineering* 35, no. 12 (2022): 2291-2296. https://doi.org/10.5829/ije.2022.35.12c.03

[31] Kunalan, Kerishmaa Theavy. "A PERFORMANCE INVESTIGATION OF A MULTI STAGED HYDROKINETIC TURBINE FOR RIVER FLOW." (2021). https://doi.org/10.37934/progee.17.1.1731

[32] Xiao, Caiyuan, Nourbakhsh, Mansour, Alizadeh, As'ad, Toghraie, Davood, Barnoon, Pouya, and Khan, Afrasyab. "Investigation of thermal behavior and performance of different microchannels: A case study for traditional and Manifold Microchannels." *Case Studies in Thermal Engineering 39*, (2022): 102393. https://doi.org/10.1016/j.csite.2022.102393

[33] Sundaram, Indira, and Srinivasa Raju Rallabandi. "Analytical Study of MHD Mixed Convection Flow for Maxwell Nanofluid Through a Vertical Cone with Porous Material in the Presence of Variable Thermal Conductivity and Soret, Dufour Effects." *Journal of Advanced Research in Fluid Mechanics and Thermal Sciences* 106, no. 2 (2023): 129-142. https://doi.org/10.37934/arfmts.106.2.129142

[34] Mukhopadhyay, Swati. "Heat transfer analysis of the unsteady flow of a Maxwell fluid over a stretching surface in the presence of a heat source/sink." *Chinese Physics Letters* 29, no. 5 (2012): 054703. https://doi.org/10.1088/0256-307X/29/5/054703

[35] Rahbari, Alireza, Morteza Abbasi, Iman Rahimipetroudi, Bengt Sundén, Davood Domiri Ganji, and Mehdi Gholami. "Heat transfer and MHD flow of non-newtonian Maxwell fluid through a parallel plate channel: analytical and numerical solution." *Mechanical Sciences* 9, no. 1 (2018): 61-70. https://doi.org/10.5194/ms-9-61-2018

[36] Khan, Zeeshan, Haroon Ur Rasheed, Tawfeeq Abdullah Alkanhal, Murad Ullah, Ilyas Khan, and Iskander Tlili. "Effect of magnetic field and heat source on upper-convected-maxwell fluid in a porous channel." *Open Physics* 16, no. 1 (2018): 917-928. https://doi.org/10.1515/phys-2018-0113

[37] Hayat, T., Z. Abbas, and M. Sajid. "Series solution for the upper-convected Maxwell fluid over a porous stretching plate." *Physics Letters A* 358, no. 5-6 (2006): 396-403. https://doi.org/10.1016/j.physleta.2006.04.117

[38] Hayat, T., C. Fetecau, and M. Sajid. "On MHD transient flow of a Maxwell fluid in a porous medium and rotating frame." *Physics letters A* 372, no. 10 (2008): 1639-1644. https://doi.org/10.1016/j.physleta.2007.10.036

[39] Raftari, Behrouz, and Ahmet Yildirim. "The application of homotopy perturbation method for MHD flows of UCM fluids above porous stretching sheets." *Computers & Mathematics with Applications* 59, no. 10 (2010): 3328-3337. https://doi.org/10.1016/j.camwa.2010.03.018

[40] Khan, Ilyas, Farhad Ali, Samiulhaq, and Sharidan Shafie. "Exact Solutions for Unsteady Magnetohydrodynamic oscillatory flow of a maxwell fluid in a porous medium." *Zeitschrift für Naturforschung A* 68, no. 10-11 (2013): 635-645. https://doi.org/10.5560/zna.2013-0040

[41] Jhankal, Anuj Kumar. "Application of homotopy perturbation method for MHD boundary layer flow of an upper-convected Maxwell fluid in a porous medium." *Chemical Engineering Research Bulletin* 18, no. 1 (2015). https://doi.org/10.3329/cerb.v18i1.26216

[42] Bakar, Shahirah Abu, Norihan Md Arifin, and Ioan Pop. "Stability Analysis on Mixed Convection Nanofluid Flow in a Permeable Porous Medium with Radiation and Internal Heat Generation." *Journal of Advanced Research in Micro and Nano Engineering* 13, no. 1 (2023): 1-17.

[43] Fathollahi, Reza, As'ad Alizadeh, Parmida Kamaribidkorpeh, Azher M. Abed, and Pooya Pasha. "Analyzing the effect of radiation on the unsteady 2D MHD Al2O3-water flow through parallel squeezing sheets by AGM and HPM." *Alexandria Engineering Journal* 69 (2023): 207-219. https://doi.org/10.1016/j.aej.2022.11.035

[44] Jalili, Payam, Ali Ahmadi Azar, Bahram Jalili, and Davood Domiri Ganji. "Study of nonlinear radiative heat transfer with magnetic field for non-Newtonian Casson fluid flow in a porous medium." *Results in Physics* 48 (2023): 106371. https://doi.org/10.1016/j.rinp.2023.106371

[45] Hayat, T., R. Sajjad, Z. Abbas, M. Sajid, and Awatif A. Hendi. "Radiation effects on MHD flow of Maxwell fluid in a channel with porous medium." *International Journal of Heat and Mass Transfer* 54, no. 4 (2011): 854-862. https://doi.org/10.1016/j.ijheatmasstransfer.2010.09.069

[46] Mabood, Fazle, Maria Imtiaz, Ahmed Alsaedi, and Tasawar Hayat. "Unsteady convective boundary layer flow of Maxwell fluid with nonlinear thermal radiation: a numerical study." *International Journal of Nonlinear Sciences and Numerical Simulation* 17, no. 5 (2016): 221-229. https://doi.org/10.1515/ijnsns-2015-0153

[47] Hosseinzadeh, Kh, M. Gholinia, B. Jafari, A. Ghanbarpour, H. Olfian, and D. D. Ganji. "Nonlinear thermal radiation and chemical reaction effects on Maxwell fluid flow with convectively heated plate in a porous medium." *Heat Transfer—Asian Research* 48, no. 2 (2019): 744-759. https://doi.org/10.1002/htj.21404

[48] Attar, M. A., M. Roshani, Kh Hosseinzadeh, and D. D. Ganji. "Analytical solution of fractional differential equations by Akbari–Ganji's method." *Partial Differential Equations in Applied Mathematics* 6 (2022): 100450. https://doi.org/10.1016/j.padiff.2022.100450

[49] Quanjin, Ma, M. N. M. Merzuki, M. R. M. Rejab, M. S. M. Sani, and Bo Zhang. "Numerical Investigation on Free Vibration Analysis of Kevlar/Glass/Epoxy Resin Hybrid Composite Laminates." *Malaysian Journal on Composites Science & Manufacturing* 9, no. 1 (2022): 11-21. https://doi.org/10.37934/mjcsm.9.1.1121OpenAccess

[50] Fallah Najafabadi, Maryam, Hossein Talebi Rostami, Khashayar Hosseinzadeh, and Davood Domiri Ganji. "Hydrothermal study of nanofluid flow in channel by RBF method with exponential boundary conditions." *Proceedings of the Institution of Mechanical Engineers, Part E: Journal of Process Mechanical Engineering* (2022): 09544089221133909. https://doi.org/10.1177/09544089221133909

[51] Najafabadi, M. Fallah, H. TalebiRostami, Kh Hosseinzadeh, and D. D. Ganji. "Investigation of nanofluid flow in a vertical channel considering polynomial boundary conditions by Akbari-Ganji's method." *Theoretical and Applied Mechanics Letters* 12, no. 4 (2022): 100356. https://doi.org/10.1016/j.taml.2022.100356

[52] Fathollahi, Reza, As' ad Alizadeh, Yaghub Safari, Hossein Nabi, Mahmoud Shamsborhan, and Fariborz Taghinia. "Examination of bio convection with nanoparticles containing microorganisms under the influence of magnetism fields on vertical sheets by five-order Runge-Kutta method." *Heliyon* 9, no. 5 (2023). https://doi.org/10.1016/j.heliyon.2023.e15982

[53] Hasibi, A., A. Gholami, Z. Asadi, and D. D. Ganji. "Investigation for brownian motion of nonlinear thermal bioconvective SPF in a nanofluid utilizing AGM method." *Physics Open* 16 (2023): 100161. https://doi.org/10.1016/j.physo.2023.100161

[54] Jalili, Bahram, Amirhossein Rezaeian, Payam Jalili, Fathollah Ommi, and Davood Domiri Ganji. "Numerical modeling of magnetic field impact on the thermal behavior of a microchannel heat sink." *Case Studies in Thermal Engineering* 45 (2023): 102944. https://doi.org/10.1016/j.csite.2023.102944

[55] He, Ji-Huan. "Homotopy perturbation technique." *Computer methods in applied mechanics and engineering* 178, no. 3-4 (1999): 257-262. https://doi.org/10.1016/S0045-7825(99)00018-3

[56] He, Ji-Huan. "Homotopy perturbation method for solving boundary value problems." *Physics letters A* 350, no. 1-2 (2006): 87-88. https://doi.org/10.1016/j.physleta.2005.10.005

[57] He, Ji-Huan. "Recent development of the homotopy perturbation method." (2008): 205-209. https://doi.org/tmna/1463150264

[58] Sanela, J., Taza Gul, S. Islam, M. A. Khan, and R. Ali Shah. "Flow of Unsteady Second Grade Fluid between Two Vertical Plates when one of the Plate Oscillating and other is stationary." *J. Appl. Environ. Biol. Sci* 4, no. 12 (2014): 41-52.

[59] VS, Sampath Kumar, and Nithyananda P. Pai. "Suction and injection effect on flow between two plates with reference to Casson fluid model." *Multidiscipline Modeling in Materials and Structures* 15, no. 3 (2018): 559-574. http://doi.org/10.1108/MMMS-05-2018-0092

[60] Moallemi, N., I. Shafieenejad, and A. Novinzadeh. "Exact solutions for flow of a Sisko fluid in pipe." *Bulletin of the Iranian Mathematical Society* 37, no. 2 (2011): 49-60.